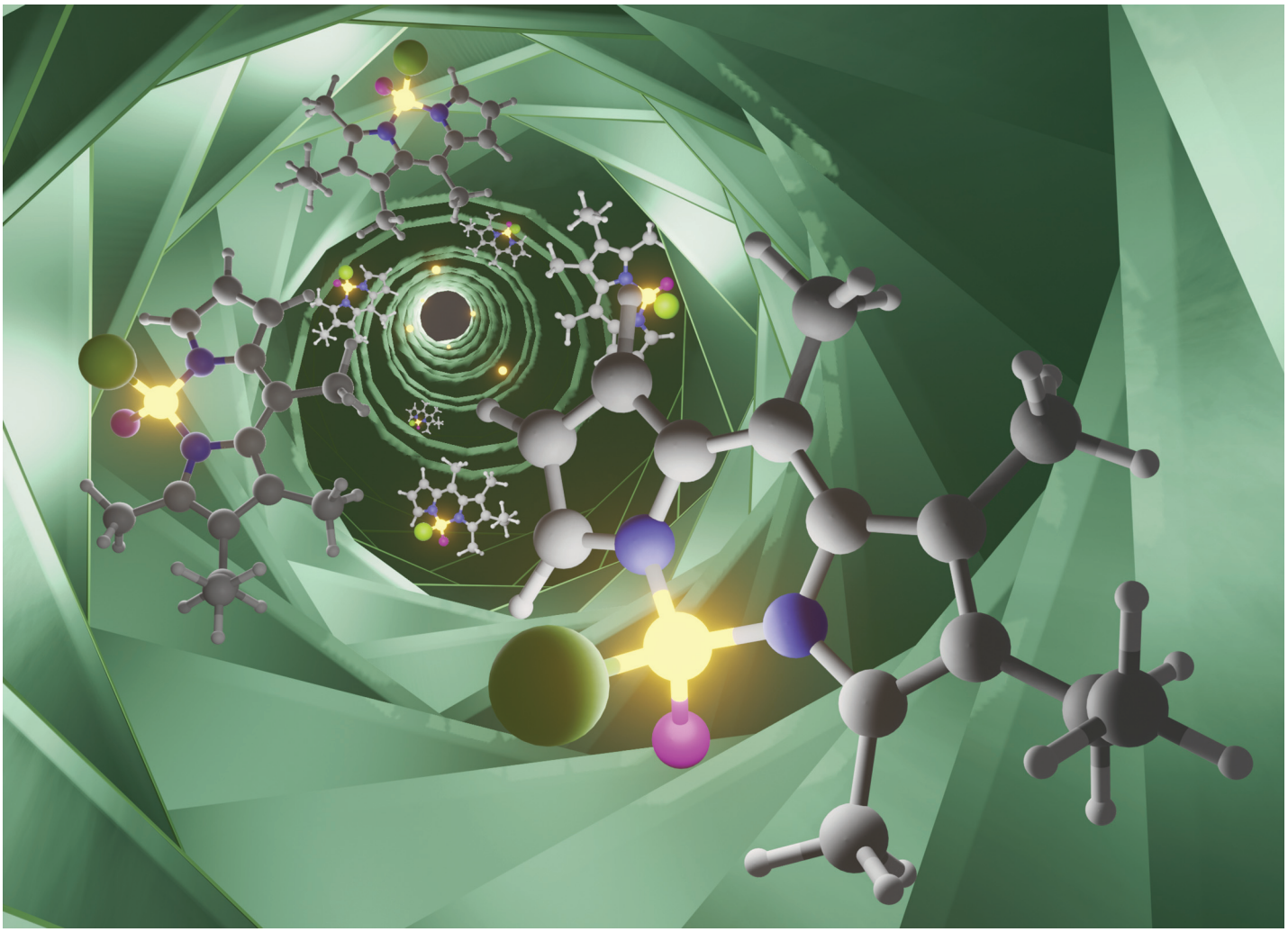

Showcasing research from Professor de la Moya's laboratory, Department of Organic Chemistry, Complutense University of Madrid, Madrid, Spain.

Dissimilar-at-boron *N*-BODIPYs: from light-harvesting multichromophoric arrays to CPL-bright *chiral-at-boron* BODIPYs

De la Moya's group describes a new BODIPY post-functionalization approach characterized by its ease and minimal photophysical interference, which allows acceleration of the design and synthesis of functional BODIPY dyes and materials, including unprecedented highly-bright chiral-at-boron BODIPYs enabling circularly polarized luminescence.

As featured in:

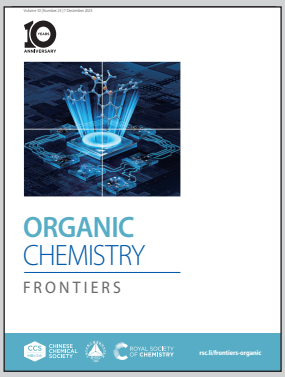

See Beatriz L. Maroto, Santiago de la Moya *et al.*, *Org. Chem. Front.*, 2023, **10**, 5834.

CCS 中国化学会 CHINESE CHEMICAL SOCIETY
SIOC 1950
ROYAL SOCIETY OF CHEMISTRY
rsc.li/frontiers-organic

ORGANIC CHEMISTRY FRONTIERS

RESEARCH ARTICLE

View Article Online
View Journal | View Issue

Cite this: *Org. Chem. Front.*, 2023, **10**, 5834

Dissimilar-at-boron *N*-BODIPYs: from light-harvesting multichromophoric arrays to CPL-bright *chiral-at-boron* BODIPYs†

César Ray,[a] Edurne Avellanal-Zaballa,[b] Mónica Muñoz-Úbeda,[c,d] Jessica Colligan,[e] Florencio Moreno,[a] Gilles Muller,[e] Iván López-Montero,[c,d,f] Jorge Bañuelos,[b] Beatriz L. Maroto *[a] and Santiago de la Moya *[a]

Received 22nd September 2023,
Accepted 9th October 2023

DOI: 10.1039/d3qo01561k

rsc.li/frontiers-organic

We report a workable and easy approach for the direct post-multifunctionalization of common BODIPYs (*F*-BODIPYs) with minimal interference to the starting photophysical behavior. It entails the easy transformation of an *F*-BODIPY into the corresponding *N*-BODIPY by using a dissimilarly-*N*,*N*′-disubstituted bis(sulfonamide), which is easily obtained from ethane-1,2-diamine. This approach is exemplified by the rapid synthesis of a selected battery of unprecedented dissimilar-at-boron *N*-BODIPYs, which are rationally designed to act as efficient multichromophoric arrays for light harvesting by excitation energy transfer, as specific bioprobes for fluorescent imaging, or as efficient chiroptical dyes exhibiting visible circular dichroism and circularly polarized luminescence. Noticeably, this approach has led to the synthesis of the first CPL-bright chiral-at-boron BODIPYs, a significant novelty in BODIPY chemistry and CPL emitters.

Introduction

The development of advanced organic dyes for sought-after photonic applications, from energy to health, has experienced exponential growth in the last few years. This is due to the inherent benefits of organic dyes and materials based on them. They exhibit a number of advantages derived from their organic nature and small molecular size, such as flexibility, lightness, membrane permeability or biocompatibility, and have the key advantages of easy synthesis and modulation by workable organic chemistry.[1]

However, today's organic photonics increasingly demands sophisticated dyes that have a wide number of different properties (*e.g.*, fluorescence, reactive oxygen species (ROS) photogeneration, biocompatibility and biospecificity for phototheragnosis[1,2]), including challenging ones such as bright circularly polarized luminescence (CPL)[3,4] (*e.g.*, to develop highly efficient CP-OLEDs *vs.* conventional OLEDs[5]). In fact, CPL organic materials are considered as next-generation materials.[6]

The post-functionalization versatility of the outstanding BODIPY (boron dipyrromethene) dyes is virtually ideal for achieving this goal,[7,8] including the generation of bright CPL.[9,10] Nevertheless, easily endowing photophysically-optimized BODIPYs with the additional properties required for a specific application is still challenging. Thus, in most cases, this post-multifunctionalization involves low-efficiency linear synthetic pathways, and the optimized starting photophysical behavior is usually affected during the functionalization process.[11] Hence, the development of easy and direct (convergent) post-multifunctionalization strategies for BODIPYs, without causing significant photophysical interference, is pivotal to advance BODIPY chemistry and organic photonics.

Among the well-established BODIPY post-functionalization approaches,[7a,11,12] those involving reactions at the boron center (mainly halogen substitutions) must be highlighted.[10b,11,12b,13–15] The significance of post-functionalization at boron is the low influence on the dye photophysics, because the boron atom is not substantial part of the BODIPY

[a]*Depto. de Química Orgánica, Facultad de CC. Químicas, Universidad Complutense de Madrid, Ciudad Universitaria s/n, 28040 Madrid, Spain. E-mail: santmoya@ucm.es, belora@ucm.es*
[b]*Depto. de Química Física, Universidad del Pais Vasco-EHU, Apartado 644, 48080 Bilbao, Spain*
[c]*Instituto de Investigación Biomédica Hospital Doce de Octubre (imas12), Avda. de Córdoba s/n, 28041 Madrid, Spain*
[d]*Departamento de Química Física, Facultad de Ciencias Químicas, Universidad Complutense de Madrid, Ciudad Universitaria s/n, 28040 Madrid, Spain*
[e]*Department of Chemistry, San José State University, San José, CA 95192-0101, USA*
[f]*Instituto Pluridisciplinar, Universidad Complutense de Madrid, Paseo de Juan XXIII 1, 28040 Madrid, Spain*

†Electronic supplementary information (ESI) available: Experimental procedures, dye characterization and supplementary tables and figures. CCDC 2269820. For ESI and crystallographic data in CIF or other electronic format see DOI: https://doi.org/10.1039/d3qo01561k

chromophore (localized at the π-conjugated dipyrrin moiety).[16] Interestingly, this approach has succeeded in easily endowing BODIPYs with valuable CPL, mainly through BINOL-based *O*-BODIPYs (involving a BO_2 moiety)[13a–c] or more-sustainable terpene-based *C*-BODIPYs (involving a BC_2 moiety).[14c] However, building dissimilar-at-boron BODIPYs (*i.e.*, BODIPYs having two different moieties dangling from the boron atom) has been scarcely used for BODIPY multifuncionalization.[17a] This is probably due to the lack of efficient procedures for the substitution of only one of the groups attached to the boron.[17] As a notable example, Harriman and Ziessel rationally developed dissimilar-at-boron *C*-BODIPYs as multichromophoric arrays for electronic energy transfer, where two different chromophores were attached to the boron atom.[17a]

Moreover, dissimilar-at-boron BODIPYs based on asymmetrically-substituted BODIPY cores present a chiral boron (chiral-at-boron BODIPYs). This would ideally lead to significant chiroptical behaviors, due to the closeness of the chiral boron to the BODIPY chromophore. With this idea in mind, Ziessel,[18a] and Işık and Tanyeli[18b] reported the few examples of chiral-at-boron BODIPYs based on *C*- and *O*-BODIPY, respectively. Unfortunately, these dyes showed low or even silent fluorescence, probably due to enhanced vibrational relaxation and intersystem crossing.[18b]

In the engaging and yet rather unexplored field of at-boron BODIPY functionalization,[11,12b] our group described in 2017 a simple methodology to synthesize the first stable *N*-BODIPYs (involving a BN_2 moiety), from accessible bis(sulfonamide)s derived from ethane-1,2-diamine (*e.g.*, see **NBDP-1** in Fig. 1).[19]

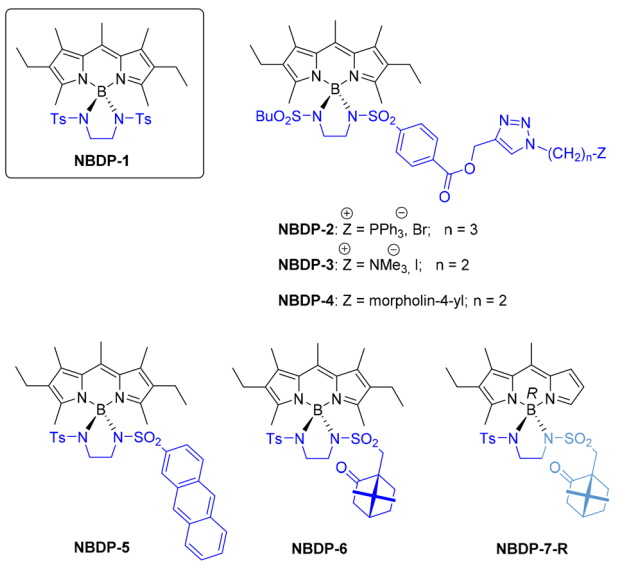

Fig. 1 Seminal *N*-BODIPY **NBDP-1**. First dissimilar-at-boron *N*-BODIPYs (**NBDP-2** and **NBDP-3**; PDT agents). Selected set of new dissimilar-at-boron *N*-BODIPYs [**NBDP-4**, **NBDP-5**, **NBDP-6** and **NBDP-7** (only the epimer **NBDP-7-R**, with an *R* configuration for boron, is shown)], rationally designed to exhibit specific functions (fluorescence, biospecificity, chiroptical behavior including CPL, differential solubility, and FRET) towards valuable photonic applications (light harvesting, bioprobing or CP lighting). Ts: tosyl (*p*-toluenesulfonyl).

These new BODIPYs are particularly important because of their demonstrated excellent photophysical signatures, which even surpass those of parent *F*-BODIPYs (*e.g.*, laser emission),[19] and also due to the possibility of BODIPY post-multifunctionalization, since up to two different moieties could be introduced at boron this way. This possibility has been preliminarily demonstrated by us through the successful preparation of *N*-BODIPYs **NBDP-2** and **NBDP-3** (Fig. 1), as potential photodynamic therapy (PDT) agents based on specific organelle accumulation, where one of the sulfonylamino moieties dangling from boron was rationally selected to gain the desired biospecificity, and the other one to address solubility issues.[20]

These preliminary results on the construction of dissimilar-at-boron *N*-BODIPYs as a versatile BODIPY post-multifunctionalization approach prompted us to investigate its scope by the rationally-guided design and efficient (convergent) synthesis of a selected set of dissimilar-at-boron *N*-BODIPYs (see Fig. 1). The dyes in this battery were designed to act as a highly fluorescent lysosome bioprobe (**NBDP-4**), as an efficient light-harvesting multichromophoric array based on workable Förster resonance energy transfer (FRET) (**NBDP-5**), as an efficient chiroptical BODIPY based on sustainable camphor (**NBDP-6**) and, which is more in the forefront, as the first highly fluorescent chiral-at-boron BODIPY (**NBDP-7**). Additionally, the selection of these dyes was made on the basis of using available starting materials to reach synthetically simple and low-cost dyes.

Results and discussion

As expected, the functionally-designed dissimilar-at-boron *N*-BODIPY dyes **NBDP-5**, **NBDP-6** and **NBDP-7** were easily obtained from the corresponding *F*-BODIPY and bis(sulfonamide) (see the reaction scheme in Table 1), following the general procedure originally developed by us for the preparation of *N*-BODIPYs equally substituted at boron.[19] This procedure uses a mixture of BCl_3/Et_3N to promote the nucleophilic substitution of the *F*-BODIPY fluorines under soft reaction conditions (see the scheme in Table 1 and the ESI† for experimental details). As the starting *F*-BODIPYs, we selected highly fluorescent and accessible ones, specifically symmetrically substituted 2,6-diethyl-1,3,5,7,8-pentamethyl-*F*-BODIPY (**FBDP-1**, a commercial laser dye known as PM567) for **NBDP-5** and **NBDP-6**, and asymmetrically substituted 2-ethyl-1,3,8-trimethyl-*F*-BODIPY (**FBDP-2**[21]) for chiral-at-boron **NBDP-7**. Regarding the intermediate bis(sulfonamide)s, **I-1** for the synthesis of **NBDP-5** and **I-2** for the synthesis of **NBDP-6** and **NBDP-7**, they were easily prepared by reacting commercially available ethane-1,2-diamine with one equivalent of *p*-toluenesulfonyl chloride in a basic medium, followed by a second analogous reaction with anthracene-2-sulfonyl chloride for **I-1** or (1*S*)-camphor-10-sulfonyl chloride for **I-2** (65% and 78% yields, respectively; see Table 1 and the ESI† for experimental details).

Table 1 Synthesis of dissimilar-at-boron *N*-BODIPYs from *F*-BODIPYs

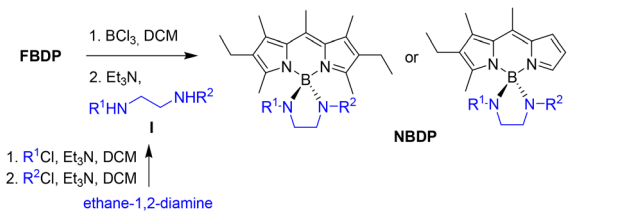

F-BODIPY[a]	R^1 [b]	R^2 [b]	I (yield)[c]	*N*-BODIPY (yield)[d]
FBDP-1	a	c	**I-1** (65%)	**NBDP-5** (35%)
FBDP-1	a	d	**I-2** (78%)	**NBDP-6** (78%)
FBDP-1	b	e	**I-3** (87%)[e]	**NBDP-8** (72%)[e]
FBDP-2	a	d	**I-2** (78%)	**NBDP-7-R** (37%)
				NBDP-7-S (39%)

DCM: dichloromethane [a] **FBDP-1**: 2,6-diethyl-1,3,5,7,8-pentamethyl-*F*-BODIPY; **FBDP-2**: 2-ethyl-1,3,8-trimethyl-*F*-BODIPY. [b] a: Tosyl; b: butane-1-sulfonyl; c: anthracene-2-sulfonyl; d: (1*S*)-camphor-10-sulfonyl; e: {4-[(propargyloxy)carbonyl]phenyl}sulfonyl. [c] Chemical yield in the preparation of **I** from ethane-1,2-diamine. [d] Chemical yield in the preparation of the *N*-BODIPY (**NBDP**) from the corresponding *F*-BODIPY (**FBDP**) and bis(sulfonamide) **I**. [e] Ref. 20.

The chemical yields for the synthesis of *N*-BODIPYs from *F*-BODIPYs (Table 1) ranged from 35% for **NBDP-5** to 78% for **NBDP-7**. Poor solubility of **I-1** in the reaction media, caused by the anthryl moiety, should explain the low yield achieved in the preparation of **NBDP-5**. In the case of **NBDP-7**, the formed epimers **NBDP-7-R** (*R* configuration for boron; see Fig. 1) and **NBDP-7-S** (*S* for boron) were easily separated by simple elution chromatography in 37% and 39% yields, respectively (see experimental details in the ESI†), and their absolute configurations were determined by X-ray diffraction analysis (see Table S3 and Fig. S4 in the ESI†).

Finally, dissimilar-at-boron *N*-BODIPY **NBDP-4** was obtained following the same procedure used preliminarily by us for the preparation of **NBDP-2** and **NBDP-3**.[20] This procedure involves first preparing the clickable ethynyl-based dissimilar-at-boron **NBDP-8** [20] from **FBDP-1** and bis(sulfonamide) **I-3** (see Table 1) to subsequently conduct a standard click reaction ($CuSO_4$/sodium ascorbate) with the corresponding functionalized azide carrying the morpholino moiety (see Fig. 2). In the case of **NBDP-4**, the click reaction of **NBDP-8** with the commercial morpholine-based azide took place in 85% chemical yield (see experimental details in the ESI†). It must be highlighted here

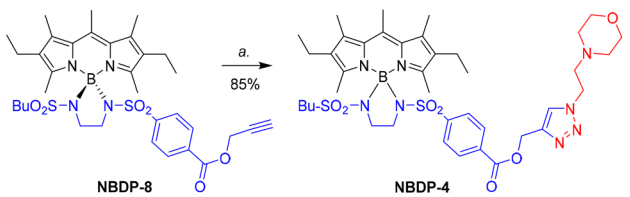

Fig. 2 Synthesis of **NBDP-4** from the previously-developed dissimilar-at-boron clickable *N*-BODIPY **NBDP-8**[20] by a click reaction. *a.* 4-(2-Azidoethyl)morpholine, $CuSO_4{\cdot}5H_2O$, sodium ascorbate, *t*-butanol/H_2O.

that using the butane-1-sulfonyl-derived bis(sulfonamide) **I-3** (instead of *p*-toluenesulfonyl) facilitated the synthesis of **NBDP-8**, probably due to the observed enhanced solubility in the reaction medium (dichloromethane). This supports the feasibility of simply using one of the at-boron pending sulfonylamino groups to modulate dye solubility, which is an important property for in-solution applications and dye material processing.

All these synthetic results, including our preliminary ones,[20] demonstrate the ease and versatility of constructing dissimilar-at-boron *N*-BODIPYs, as well as the utility of **NBDP-8** (and related compounds) as a readily-accessible precursor of functionalized BODIPY dyes through workable click chemistry.

Regarding ground state photophysics, the recorded visible spectral signatures (see the ESI† for experimental details) of all the obtained PM567-derived dissimilar-at-boron *N*-BODIPYs, including preliminary **NBDP-8**, **NBDP-2** and **NBDP-3**,[20] closely resemble those reported for related both **NBDP-1**[19] (equally substituted at boron) and parent *F*-BODIPY **FBDP-1** (see Table 2 and Fig. S1†). As expected, the unequal substitution of the starting *F*-BODIPY fluorines with different nitrogenated moieties does not affect the fluorescence capacity of the dissimilar-at-boron *N*-BODIPY dyes. They all exhibit fluorescence quantum yields higher than 80%, regardless of the solvent used for the measurement, with only slight bathochromic shifts (less than 10 nm) and some small changes in the absorption coefficient, together with a moderate increase in the lifetime (see Table 2, and Table S1 in the ESI†). The same behavior is found for chiral-at-boron *N*-BODIPYs **NBDP-7-R** and **NBDP-7-S**, which exhibit fluorescence signatures closely related to those of the corresponding parent *F*-BOPIPY **FBDP-2**,

Table 2 Ground state visible photophysical signatures of the designed set of dissimilar-at-boron *N*-BODIPYs (**NBDP-4**, **NBDP-5**, **NBDP-6** and **NBDP-7** epimers), including preliminary ones **NBDP-2**, **NBDP-3** and **NBDP-8**[20] (see Fig. 1), equally disubstituted *N*-BODIPY **NBDP-9** (see Fig. 5), and parent *F*-BODIPYs **FBDP-1** and **FBDP-2** (see Table 1), in methanol (*ca.* 2×10^{-6} M). Previously reported data for **NBDP-1**[19] (see Fig. 1) are included for comparison purposes. For data in other solvents, see Table S1 in the ESI†

Dye	λ_{ab} [a] (nm)	ε_{max} [b] ($10^4 \times M^{-1}cm^{-1}$)	λ_{fl} [c] (nm)	ϕ [d]	τ [e] (ns)
FBDP-1	516.0	7.9	532.0	0.91	6.10
NBDP-1	525.5	6.2	542.0	0.82	8.37
NBDP-2	524.5	5.1	544.0	0.80	7.77
NBDP-3	524.5	5.2	541.5	0.73	7.76
NBDP-4	524.5	5.5	543.5	0.88	7.82
NBDP-5	522.5	6.2	538.0	0.80	7.93
NBDP-6	524.0	5.6	541.5	0.82	8.31
NBDP-8	524.5	6.0	542.5	0.80	8.16
NBDP-9	523.0	5.5	542.0	0.93	8.28
FBDP-2	495.5	4.3	510.5	0.80	5.80
NBDP-7-R	504.5	2.8	520.5	0.87	8.00
NBDP-7-S	502.5	2.6	519.5	0.82	7.56

[a] Maximum absorption wavelength. [b] Maximum molar absorption coefficient. [c] Maximum fluorescence wavelength. [d] Fluorescence quantum yield. [e] Fluorescence lifetime.

with the exception of some loss of absorption capability (see Table 2).

Importantly, the strong fluorescence emission recorded for **NBDP-7-R** and **NBDP-7-S**, with fluorescence quantum yields up to *ca.* 90% in methanol (see Table 2), makes them the first highly fluorescent chiral-at-boron BODIPYs reported so far, a significant record in chiral-BODIPY chemistry and photonics.

Regarding the FRET-based light-harvesting behavior designed for **NBDP-5**,[13d,22] the UV-Vis absorption spectrum of this dye shows the two expected absorption bands: a sharp one that peaked at 530 nm, with higher intensity, ascribed to the BODIPY chromophore, and another one, broader and weaker, centered at 370 nm, featuring the typical resolved vibrational resolution of anthracene absorption[22a] (Fig. 3).

As designed, the fluorescence spectrum of **NBDP-5** shows a single band regardless of the used irradiation wavelength, 530 nm for BODIPY chromophore excitation or 370 nm for anthracene chromophore excitation (Fig. 3). Moreover, the corresponding excitation spectrum, monitored at the long-wavelength tail of the fluorescence profile (620 nm), fully matches the absorption one, supporting electronic isolation for the involved anthracene and BODIPY chromophores. All these results demonstrate excitation-energy transfer (EET) from the anthracene moiety (energy donor) to the BODIPY one (energy acceptor), with *ca.* 100% EET efficiency, as calculated from the loss of anthracene-chromophore fluorescence (residual donor emission in **NBDP-5** is almost negligible upon its direct excitation; see the ESI†). Possible competing electron-transfer between the acting chromophores was ruled out by electrochemical measurements, since the main oxidation and reduction bands in the cyclic voltammogram of **NBDP-5** match those of isolated **FBDP-1** and anthracene (see Fig. S2 in the ESI†). Besides, FRET[23a] must be the mechanism involved in the observed EET process, as supported by the spectral overlapping between the anthracene-chromophore emission and the BODIPY-chromophore absorption (see Fig. S3 in the ESI†), enabling the required dipole–dipole coupling. Besides, the at-boron linkage hampers any electronic exchange by the through-bond mechanism;[23b] however, it brings both acting chromophores close to each other (the B3LYP/6-311g* computed distance between their centers of masses is 8.3 Å; see Fig. S3 in the ESI†), allowing efficient through-space mediated EET.[23c] All these photophysical, electrochemical and computational results demonstrate the usefulness of constructing dissimilar-at-boron *N*-BODIPYs to develop valuable light-harvesting organic dyes.

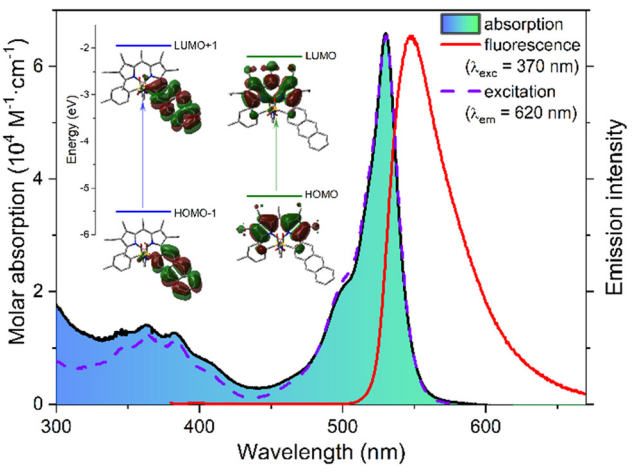

Fig. 3 UV-Vis absorption, and normalized fluorescence and excitation spectra of **NBDP-5** in cyclohexane (*ca.* 2×10^{-6} M). The corresponding contour maps of the frontier molecular orbitals computed as involved in the main UV and Vis transitions (B3LYP/6-311g*) are included.

In relation to the lysosomal probing behavior designed for **NBDP-4**, it must be noted that this dye has a basic morpholine moiety, which is known to promote specific accumulation in acidic lysosomes.[24] Moreover, as in the case of preliminary **NBDP-2** and **NBDP-3**,[20] the involved molecular arrangement comprises a number of advantageous features for fluorescence bioprobing. On the one hand, the moiety responsible for the biospecificity is located far from the one responsible for the fluorescence signaling (the BODIPY core) and, therefore, no interference is expected from either photophysics or biospecificity viewpoints. On the other hand, their easy synthetic access from a common reactive intermediate (**NBDP-8**, see Fig. 2) facilitates not only the rapid generation of different bioprobes (labelling different biosystems), but also the rapid synthesis of related ones (labelling the same biosystem) for bioprobe optimization purposes.

As expected, highly fluorescent morpholine-based **NBDP-4** effectively functions as a specific lysosomal bioprobe. This was assessed in living mouse embryonic fibroblasts (MEFs), which were stained simultaneously with LysoTracker™ Red (4 nM) and **NBDP-4** (500 nM) (see the ESI† for experimental details). Co-localization of both probes was imaged by fluorescence confocal scanning laser microscopy (CSLM; see the ESI† for experimental details). Although **NBDP-4** was detected within the cellular cytoplasm as a dim fluorescent background, this *N*-BODIPY dye strongly co-localized with Lysotracker™ Red even with short incubation times. The calculated Pearson's coefficient (R) was above the threshold for high colocalization, with values equal to 0.93, 0.93 and 0.94 for incubation times of 30 min, 1 h and 2 h, respectively (Fig. 4). These biophotophysical results, together with the preliminary ones reported by us for **NBDP-2** and **NBDP-3**,[20] demonstrate the high capability of the involved dissimilar-at-boron *N*-BODIPY design for cellular uptake and specific fluorescence probing, as well as the workability of **NBDP-8** to rapidly build subcellular fluorescent bioprobes.

Regarding the chiroptical behavior designed for **NBDP-6** and epimers **NBDP-7-R** and **NBDP-7-S**, these dyes exhibit the expected visible electronic circular dichroism (ECD) in diluted chloroform solution (see the ESI† for experimental details), due to the chiral perturbation of the BODIPY chromophore caused by the involved chiral elements. However, the dichroic capability of **NBDP-6** is significantly poorer than that exhibited by **NBDP-7-R** and **NBDP-7-S**, as measured using the corres-

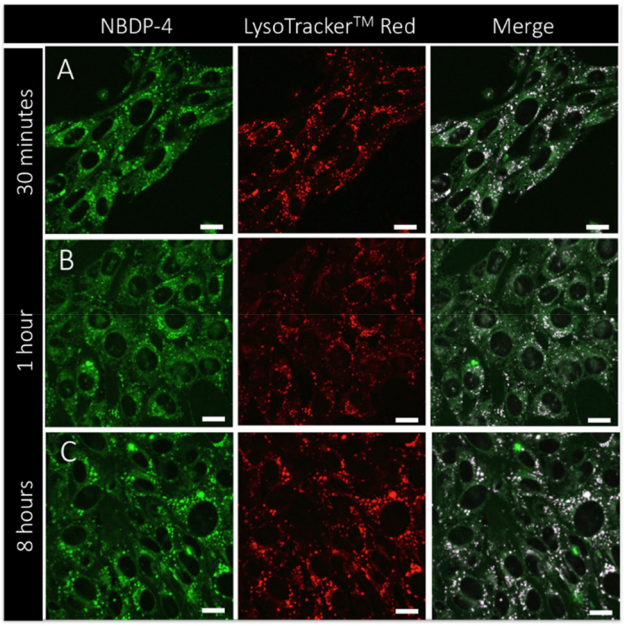

Fig. 4 Green- and red-channel merged CLSM images of lysosomes in living MEFs co-stained with green **NBDP-4** (500 nM) and LysoTracker™ Red (4 n M), respectively. MEFs were imaged after 30 minutes of incubation (A), after 1 h of incubation (B) and after 8 h of incubation (C). Green channel: λ_{exc} = 488 nm and λ_{em} = 525 ± 25 nm. Red channel: λ_{exc} = 561 nm and λ_{em} > 561 nm. Scale bars are 10 μm.

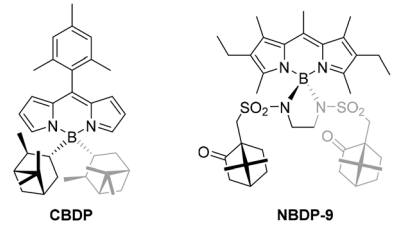

Fig. 5 Related C_2-symmetric BODIPYs functionalized at boron with hanging chiral terpene moieties: known isopinocampheyl-based *C*-BODIPY **CBDP**[14c] and camphor-based *N*-BODIPY **NBDP-9**.

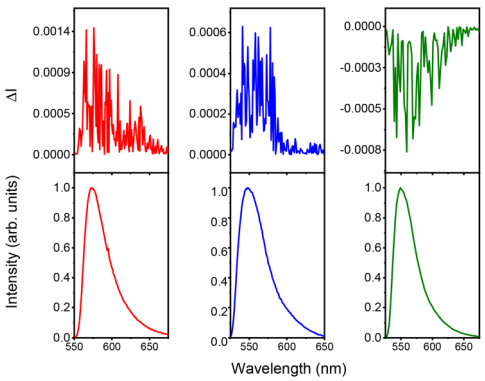

Fig. 6 CPL (upper curves) and total luminescence (lower curves) spectra of **NBDP-9** (red), **NBDP-7-R** (blue) and **NBDP-7-S** (green) in degassed chloroform (1 mM).

ponding calculated maximum $|g_{abs}$‡$|$ (0.1×10^{-3} for **NBDP-6** *vs.* 1.4×10^{-3} and 1.2×10^{-3} for **NBDP-7-R** and **NBDP-7-S**; see Table S2 in the ESI†). This suggests low chiral-perturbing capability from the hanging chiral camphor moiety, and higher from the chiral boron center (note the change of the g_{abs} sign when changing the boron configuration in **NBDP-7** epimers; Table S2 in the ESI†). The reason must be the high conformational mobility and long distance to the BODIPY chromophore of the camphor moiety, compared to the closer and conformationally-fixed chiral boron center. To prove the low perturbing capability of the camphor moiety in this structure, we decided to synthesize and chiroptically characterize C_2-symmetric **NBDP-9** (Fig. 5; see the ESI†), in order to compare it to known related **CBDP**,[14c] which has conformationally-restricted chiral terpene moieties located closer to the BODIPY chromophore (*cf.* **CBDP** and **NBDP-9** in Fig. 5).

Satisfactorily, **NBDP-9** exhibited the characteristic, excellent fluorescence signatures of the *N*-BODIPY family (see Table 2, and Table S1 in the ESI†). However, regarding chiroptics, while terpene-based *C*-BODIPY **CBDP** was reported to be ECD-active in the Vis region,[14c] related *N*-BODIPY **NBDP-9** turned out to be ECD-silent under almost the same experimental conditions (see Table S2 in the ESI†). This result supports the hypothesis mentioned above on the low chiral-perturbing capability of the distant and moving terpene moieties of the developed camphor-based *N*-BODIPY dyes.

Regarding visible CPL, all the synthesized camphor-based BODIPYs are CPL active, including ECD-silent **NBDP-9** (*e.g.*, see the CPL spectra of **NBDP-9**, and **NBDP-7** epimers in chloroform solution in Fig. 6; see the ESI† for experimental details), with the maximum $|g_{lum}$§$|$ values ranging from *ca.* 0.5×10^{-3} for **NBDP-7-R** to *ca.* 1×10^{-3} for **NBDP-9** and **NBDP-7-S** (see Table S2 in the ESI†).

The clear CPL activity of ECD-silent **NBDP-9** could be explained by the participation of a more electronically-forbidden transition for the emission band, when compared with that for the absorption.[25] Noteworthily, for the ECD-active *N*-BODIPYs **NBDP-6**, **NBDP-7-R** and **NBDP-7-S**, the signs of the visible maximum g_{abs} and the corresponding visible maximum g_{lum} are the same (see Table S2 in the ESI†). This behavior is different to those reported for related at-boron-substituted BINOL-based *O*-BODIPYs[13a] and isopinocampheyl-based *C*-BODIPYs,[14c] and can be explained on the basis of the low probability of the investigated *N*-BODIPYs for enabling intramolecular charge transfer (ICT) emission upon light absorp-

‡The degree of ECD is given by the Kunh's dissymmetry ratio, $g_{abs}(\lambda) = 2(\varepsilon_L - \varepsilon_R)/(\varepsilon_L + \varepsilon_R)$, where ε_L and ε_R are the molar absorption coefficients of left and right circularly polarized absorption, respectively.

§The degree of CPL is given by the luminescence dissymmetry factor, $g_{lum}(\lambda) = 2(I_L - I_R)/(I_L + I_R)$, where I_L and I_R are the intensities of left and right circularly polarized emission, respectively.

tion,[26] as supported by their high fluorescence capabilities, regardless of the solvent polarity (see Table S1 in the ESI†).

Finally, it must be noted that despite the precautions that must be taken when handling g_{lum} data of small organic molecules (note the common very small values and the inherent experimental errors), significant visible g_{lum} values are obtained from the developed highly fluorescent chiral-at-boron *N*-BODIPYs **NBDP-7**, *i.e.*, having a stereogenic boron. It is true that these BODIPYs include a chiral moiety (from natural camphor) in their molecular structure, but as demonstrated before, its role is to facilitate epimer separation upon synthesis, rather than influencing the dye chiroptical activity. All these characteristics of the reported chiral-at-boron *N*-BODIPYs (high fluorescence, chirality coming from the sustainable, natural chiral pool, and CPL activity within the range of the best CPL-enabling simple organic molecules, CPL-SOMs[3b,9]) support them as the first examples of a valuable new family of chiral BODIPYs for advancing CPL BODIPYs and CPL-SOM-based materials and applications.

Conclusions

Construction of dissimilar-at-boron *N*-BODIPYs from the corresponding *F*-BODIPYs and accessible ethane-1,2-diamine-based bis(sulfonamide)s is demonstrated to be a workable new approach for easy and direct BODIPY post-multifunctionalization, with minimal perturbation of the dye ground state photophysics. Such post-multifunctionalization has great value, since it allows the rapid implementation of more than one property in a selected, photophysically-optimized BODIPY dye and should accelerate the achievement of improved BODIPYs for advancing organic photonics. This is supported by the reported rapid design and synthesis of an efficient light-harvesting multichromophoric array based on FRET, a clickable dye reagent, a lysosomal fluorescent bioprobe, and a set of chiroptical SOMs, including CPL-SOMs. Regarding chiroptics, the new approach has allowed the rapid achievement of the first highly-fluorescent chiral-at-boron BODIPYs. Their high fluorescence and their efficient CPL-activity and sustainable chirality coming from the natural chiral pool make this new family of BODIPY dyes highly interesting to advance CPL-SOMs and sought-after photonic materials and applications based of them (*e.g.*, full-organic probes for CPL bioimaging[6] or more sustainable CP-OLEDs[5]).

Author contributions

Conceptualization: B.L.M., S.d.l.M.; funding acquisition: S.d.l.M., J.B., G.M., I.L.-M.; investigation: C.R., E.A.-Z., M.M.-Ú., J.C.; methodology: B.L.M., F.M., J.B., G.M., I.L.-M.; supervision: B.L.M., F.M., J.B., G.M., I.L.-M.; writing – original draft: B.L.M., S.d.l.M., with input from all the authors; writing – review & editing: B.L.M., S.d.l.M., J.B., G.M., I.L.-M. All authors have read and agreed to the published version of the manuscript.

Conflicts of interest

There are no conflicts to declare.

Acknowledgements

This research received financial support from the Spanish Ministerio de Ciencia e Innovación (MICIN)/Agencia Estatal de Investigación PID2020-114755GB-C32 and C-33 AEI/10.13039/501100011033 and from the Basque Government (Grant IT1639-22). This work was also supported by the TECNOLOGÍAS 2018 program, funded by the Regional Government of Madrid, Spain (Grant S2018/BAA-4403 SINOXPHOS-CM, to I.L-M.). M.M.-Ú. was recipient of a Sara Borrell fellowship (CD15/00190) financed by the Spanish Ministry of Health. G.M. is thankful for the financial support by the California State University Program for Education and Research in Biotechnology (CSUPERB) Research Development Grant. C.R. thanks Comunidad de Madrid-UCM for a research contract (Programa Operativo de Empleo Juvenil, YEI).

References

1 For example, see: (*a*) B. N. G. Giepmans, S. R. Adams, M. H. Ellisman and R. Y. Tsien, The fluorescent toolbox for assessing protein location and function, *Science*, 2006, **312**, 217–224; (*b*) A. Bessette and G. S. Hanan, Design, synthesis and photophysical studies of dipyrromethene-based materials: insights into their applications in organic photovoltaic devices, *Chem. Soc. Rev.*, 2014, **43**, 3342–3405; (*c*) R. Strack, Organic dyes for live imaging, *Nat. Methods*, 2021, **18**, 30; (*d*) X. Zhang, J. Gao, Y. Tang, J. Yu, S. S. Liew, C. Qiao, Y. Cao, G. Liu, H. Fan, Y. Xia, J. Tian, K. Pu and Z. Wang, Bioorthogonally activatable cyanine dye with torsion-induced disaggregation for in vivo tumor imaging, *Nat. Commun.*, 2022, **13**, 3513; (*e*) L. Sun, Y. Chen, M. Sun and Y. Zheng, Organic Solar Cells: Physical Principle and Recent Advances, *Chem. - Asian J.*, 2023, e202300006.

2 For example, see: (*a*) S. Atilgan, T. Ozdemir and E. U. Akkaya, A Sensitive and Selective Ratiometric Near IR Fluorescent Probe for Zinc Ions Based on the Distyryl–Bodipy Fluorophore, *Org. Lett.*, 2008, **10**, 4065–4067; (*b*) G. Duran-Sampedro, A. R. Agarrabeitia, I. Garcia-Moreno, L. Gartzia-Rivero, S. de la Moya, J. Banuelos, I. Lopez-Arbeloa and M. J. Ortiz, An asymmetric BODIPY triad with panchromatic absorption for high-performance red-edge laser emission, *Chem. Commun.*, 2015, **51**, 11382–11385; (*c*) V.-N. Nguyen, Y. Yim, S. Kim, B. Ryu, K. M. K. Swamy, G. Kim, N. Kwon, C.-Y. Kim, S. Park and J. Yoon, Molecular Design of Highly Efficient Heavy-Atom-

Free Triplet BODIPY Derivatives for Photodynamic Therapy and Bioimaging, *Angew. Chem., Int. Ed.*, 2020, **59**, 8957–8962.

3 (*a*) Y. Zhang, S. Yu, B. Han, Y. Zhou, X. Zhang, X. Gao and Z. Tang, Circularly polarized luminescence in chiral materials, *Matter*, 2022, **5**, 837–875; (*b*) E. M. Sánchez-Carnerero, A. R. Agarrabeitia, F. Moreno, B. L. Maroto, G. Muller, M. J. Ortiz and S. de la Moya, Circularly Polarized Luminescence from Simple Organic Molecules, *Chem. – Eur. J.*, 2015, **21**, 13488–13500; (*c*) J. Kumar, T. Nakashima and T. Kawai, Circularly Polarized Luminescence in Chiral Molecules and Supramolecular Assemblies, *J. Phys. Chem. Lett.*, 2015, **6**, 3445–3452.

4 For example, see: (*a*) K. Ma, W. Chen, T. Jiao, X. Jin, Y. Sang, D. Yang, J. Zhou, M. Liu and P. Duan, Boosting the circularly polarized luminescence of small organic molecules via multi-dimensional morphology control, *Chem. Sci.*, 2019, **10**, 6821–6827; (*b*) C. Maeda, K. Nagahata, T. Shirakawa and T. Ema, Azahelicene-Fused BODIPY Analogues Showing Circularly Polarized Luminescence, *Angew. Chem., Int. Ed.*, 2020, **59**, 7813–7817; (*c*) J.-F. Chen, Q.-X. Gao, L. Liu, P. Chen and T.-B. Wei, A pillar[5]arene-based planar chiral charge-transfer dye with enhanced circularly polarized luminescence and multiple responsive chiroptical changes, *Chem. Sci.*, 2023, **14**, 987–993.

5 (*a*) S. Feuillastre, M. Pauton, L. Gao, A. Desmarchelier, A. J. Riives, D. Prim, D. Tondelier, B. Geffroy, G. Muller, G. Clavier and G. Pieters, Design and Synthesis of New Circularly Polarized Thermally Activated Delayed Fluorescence Emitters, *J. Am. Chem. Soc.*, 2016, **138**, 3900–3993; (*b*) K. Dhbaibi, L. Abella, S. Meunier-Della-Gatta, T. Roisnel, N. Vanthuyne, B. Jamoussi, G. Pieters, B. Racine, E. Quesnel, J. Autschbach, J. Crassous and L. Favereau, Achieving high circularly polarized luminescence with push–pull helicenic systems: from rationalized design to top-emission CP-OLED applications, *Chem. Sci.*, 2021, **12**, 5522–5533.

6 (*a*) H. Koike, K. Nozaki and M. Iwamura, Microscopic Imaging of Chiral Amino Acids in Agar Gel through Circularly Polarized Luminescence of EuIII Complex, *Chem. - Asian J.*, 2020, **15**, 85–90; (*b*) P. Stachelek, L. MacKenzie, D. Parker and R. Pal, Circularly polarised luminescence laser scanning confocal microscopy to study live cell chiral molecular interactions, *Nat. Commun.*, 2022, **13**, 553.

7 (*a*) J. Zhao, K. Xu, W. Yang, Z. Wang and F. Zhong, The triplet excited state of Bodipy: formation, modulation and application, *Chem. Soc. Rev.*, 2015, **44**, 8904–8939; (*b*) H. Lu, J. Mack, T. Nyokong, N. Kobayashi and Z. Shen, Optically active BODIPYs, *Coord. Chem. Rev.*, 2016, **318**, 1–15; (*c*) J. Bañuelos, BODIPY Dye, the Most Versatile Fluorophore Ever?, *Chem. Rec.*, 2016, **16**, 335–348; (*d*) S. Kolemen and E. U. Akkaya, Reaction-based BODIPY probes for selective bio-imaging, *Coord. Chem. Rev.*, 2018, **354**, 121–134; (*e*) E. Bassan, A. Gualandi, P. G. Cozzi and P. Ceroni, Design of BODIPY dyes as triplet photosensitizers, *Chem. Sci.*, 2021, **12**, 6607–6628.

8 For example, see: (*a*) M. Chapran, E. Angioni, N. J. Findlay, B. Breig, V. Cherpak, P. Stakhira, T. Tuttle, D. Volyniuk, J. V. Grazulevicius, Y. A. Nastishin, O. D. Lavrentovich and P. J. Skabara, An Ambipolar BODIPY Derivative for a White Exciplex OLED and Cholesteric Liquid Crystal Laser toward Multifunctional Devices, *ACS Appl. Mater. Interfaces*, 2017, **9**, 4750–4757; (*b*) J. Zou, P. Wang, Y. Wang, G. Liu, Y. Zhang, Q. Zhang, J. Shao, W. Si, W. Huang and X. Dong, Penetration depth tunable BODIPY derivatives for pH triggered enhanced photothermal/photodynamic synergistic therapy, *Chem. Sci.*, 2019, **10**, 268–276; (*c*) A. Cortés-Villena, D. A. Caminos, R. E. Galian and J. Pérez-Prieto, Singlet Sensitization of a BODIPY Rotor Triggered by Marriage with Perovskite Nanocrystals, *Adv. Opt. Mater.*, 2023, 2300138.

9 M. J. Hall and S. de la Moya, BODIPY based emitters of circularly polarized luminescence, in *Circularly polarized luminescence of isolated small organic molecules*, ed. T. Mori, Springer, Singapore, 2020, pp. 117–149.

10 For example, see: (*a*) Y. Gobo, M. Yamamura, T. Nakamura and T. Nabeshima, Synthesis and Chiroptical Properties of a Ring-Fused BODIPY with a Skewed Chiral π Skeleton, *Org. Lett.*, 2016, **18**, 2719–2721; (*b*) N. Algoazy, R. G. Clarke, T. J. Penfold, P. G. Waddell, M. R. Probert, R. Aerts, W. Herrebout, P. Stachelek, R. Pal, M. J. Hall and J. G. Knight, Near-Infrared Circularly Polarised Luminescence from Helically Extended Chiral N,N,O, O-Boron Chelated Dipyrromethenes, *ChemPhotoChem*, 2022, **6**, e202200090; (*c*) C. Ray, C. Díaz-Norambuena, M. Johnson, F. Moreno, B. L. Maroto, J. Bañuelos, G. Muller and S. de la Moya, Tuning CPL by helical pitch modulation in helically flexible small organic multichromophores, *J. Mater. Chem. C*, 2023, **11**, 456–461; (*d*) L. Cui, K. Deyama, T. Ichiki, Y. Konishi, A. Horioka, T. Harada, K. Ishibashi, Y. Hisaeda and T. Ono, Color-tuning and boosting circularly polarized luminescence performance of axially chiral tetra-BF2 complexes by post-modifications, *J. Mater. Chem. C*, 2023, **11**, 2574–2581.

11 E. Bodio and C. Goze, Investigation of B-F substitution on BODIPY and aza-BODIPY dyes: Development of B-O and B-C BODIPYs, *Dyes Pigm.*, 2019, **160**, 700–710.

12 (*a*) N. Boens, B. Verbelen, M. J. Ortiz, L. Jiao and W. Dehaen, Synthesis of BODIPY dyes through postfunctionalization of the boron dipyrromethene core, *Coord. Chem. Rev.*, 2019, **399**, 213024; (*b*) R. L. Gapare and A. Thompson, Substitution at boron in BODIPYs, *Chem. Commun.*, 2022, **58**, 7351–7359.

13 For examples of BODIPYs with *O*-substitution at boron (*O*-BODIPYs), see: (*a*) E. M. Sánchez-Carnerero, F. Moreno, B. L. Maroto, A. R. Agarrabeitia, M. J. Ortiz, B. G. Vo, G. Muller and S. de la Moya, Circularly Polarized Luminescence by Visible-Light Absorption in a Chiral O-BODIPY Dye: Unprecedented Design of CPL Organic Molecules from Achiral Chromophores, *J. Am. Chem. Soc.*, 2014, **136**, 3346–3349; (*b*) S. Zhang, Y. Wang, F. Meng, C. Dai, Y. Cheng and C. Zhu, Circularly polarized lumine-

scence of AIE-active chiral O-BODIPYs induced via intramolecular energy transfer, *Chem. Commun.*, 2015, **51**, 9014–9017; (*c*) J. Jiménez, C. Díaz-Norambuena, S. Serrano, S. C. Ma, F. Moreno, B. L. Maroto, J. Bañuelos, G. Muller and S. de la Moya, BINOLated aminostyryl BODIPYs: a workable organic molecular platform for NIR circularly polarized luminescence, *Chem. Commun.*, 2021, **57**, 5750–5753; (*d*) C. O. Obondi, G. N. Lim, P. Martinez, V. Swamy and F. D'Souza, Controlling electron and energy transfer paths by selective excitation in a zinc porphyrin–BODIPY–C60 multi-modular triad, *Nanoscale*, 2017, **9**, 18054.

14 For examples of BODIPYs with *C*-substitution at boron (*C*-BODIPYs), see: (*a*) C. Uriel, A. M. Gómez, E. García Martínez de la Hidalga, J. Bañuelos, I. Garcia-Moreno and J. C. López, Access to 2,6-Dipropargylated BODIPYs as "Clickable" Congeners of Pyrromethene-567 Dye: Photostability and Synthetic Versatility, *Org. Lett.*, 2021, **23**, 6801–6806; (*b*) Y. Zhang, S. Yuan, P. Liu, L. Jing, H. Pan, X.-K. Ren and Z. Chen, J-aggregation induced emission enhancement of BODIPY dyes via H-bonding directed supramolecular polymerization: the importance of substituents at boron, *Org. Chem. Front.*, 2021, **8**, 4078–4085; (*c*) J. Jiménez, F. Moreno, T. Arbeloa, T. A. Cabreros, G. Muller, J. Bañuelos, I. García-Moreno, B. L. Maroto and S. de la Moya, Isopinocampheyl-based C-BODIPYs: a model strategy to construct cost-effective boron-chelate emitters of circularly polarized light, *Org. Chem. Front.*, 2021, **8**, 4752–4757; (*d*) Y. Zhou, Y. Gao, L. Pang, W. Kang, K. Man and W. Wang, A green light-enhanced cytosolic protein delivery platform based on BODIPY-protein interactions, *Nano Res.*, 2023, **16**, 1042–1051.

15 For examples of BODIPYs with *COO*-substitution at boron (*COO*-BODIPYs), see: (*a*) C. Ray, C. Schad, F. Moreno, B. L. Maroto, J. Bañuelos, T. Arbeloa, I. García-Moreno, C. Villafuerte, G. Muller and S. de la Moya, BCl3-Activated Synthesis of COO-BODIPY Laser Dyes: General Scope and High Yields under Mild Conditions, *J. Org. Chem.*, 2020, **85**, 4594–4601. For examples of BODIPYs with other substitutions at boron, see: (*b*) A. Blazquez-Moraleja, I. Saenz-de-Santa Maria, M. D. Chiara, D. Alvarez-Fernandez, I. Garcia-Moreno, R. Prieto-Montero, V. Martinez-Martinez, I. López Arbeloa and J. L. Chiara, Shedding light on the mitochondrial matrix through a functional membrane transporter, *Chem. Sci.*, 2020, **11**, 1052–1065; (*c*) M. Wang, G. Zhang, P. Bobadova-Parvanova, K. M. Smith and M. G. H. Vicente, Syntheses and Investigations of Conformationally Restricted, Linker-Free α-Amino Acid–BODIPYs via Boron Functionalization, *J. Org. Chem.*, 2021, **86**, 18030–18041; (*d*) C. Schad, E. Avellanal-Zaballa, E. Rebollar, C. Ray, E. Duque-Redondo, F. Moreno, B. L. Maroto, J. Bañuelos, I. García-Moreno and S. de la Moya, Triplet–triplet sensitizing within pyrene-based COO-BODIPY: a breaking molecular platform for annihilating photon upconversion, *Phys. Chem. Chem. Phys.*, 2022, **24**, 27441–27448.

16 F. López Arbeloa, J. Bañuelos, V. Martínez, T. Arbeloa and I. López Arbeloa, Structural, photophysical and lasing properties of pyrromethene dyes, *Int. Rev. Phys. Chem.*, 2005, **24**, 339–374.

17 (*a*) A. Harriman, L. Mallon, S. Goeb, G. Ulrich and R. Ziessel, Electronic Energy Transfer to the S2 Level of the Acceptor in Functionalised Boron Dipyrromethene Dyes, *Chem. – Eur. J.*, 2009, **15**, 4553–4564; (*b*) A. B. More, S. Mula, S. Thakare, N. Sekar, A. K. Ray and S. Chattopadhyay, *J. Org. Chem.*, 2014, **79**, 10981–10987.

18 (*a*) A. Haefele, C. Zedde, P. Retainlleau, G. Ulrich and R. Ziessel, Boron Asymmetry in a BODIPY Derivative, *Org. Lett.*, 2010, **12**, 1672–1675; (*b*) M. Işık, E. Dündar, E. Şahin and C. Tanyeli, A boron dipyrromethene chiral at boron and carbon with a bent geometry: synthesis, resolution and chiroptical properties, *Chem. Commun.*, 2022, **58**, 7188–7191.

19 C. Ray, L. Díaz-Casado, E. Avellanal-Zaballa, J. Bañuelos, L. Cerdán, I. García-Moreno, F. Moreno, B. L. Maroto, Í. López-Arbeloa and S. de la Moya, N-BODIPYs Come into Play: Smart Dyes for Photonic Materials, *Chem. – Eur. J.*, 2017, **23**, 9383–9390.

20 C. Ray, A. García-Sampedro, C. Schad, E. Avellanal-Zaballa, F. Moreno, M. J. Ortiz, J. Bañuelos, A. Villanueva, P. Acedo, B. L. Maroto and S. de la Moya, Alkynyl N-BODIPYs as Reactive Intermediates for the Development of Dyes for Biophotonics, *Chem. Proc.*, 2021, **3**, 15.

21 J. Bañuelos, I. Lopez-Arbeloa, I. García-Moreno, A. Costela, L. Infante, E. Perez-Ojeda, M. Palacios-Cuesta and M. J. Ortiz, Controlling Optical Properties and Function of BODIPY by Using Asymmetric Substitution Effects, *Chem. – Eur. J.*, 2010, **16**, 14094–14105.

22 For example, see: (*a*) C.-W. Wan, A. Burghart, J. Chen, F. Bergström, L. B.-Å. Johansson, M. F. Wolford, T. G. Kim, M. R. Topp, R. M. Hochstrasser and K. Burgess, Anthracene–BODIPY Cassettes: Syntheses and Energy Transfer, *Chem. – Eur. J.*, 2003, **9**, 4430–4441; (*b*) C. Ray, C. Schad, E. Avellanal-Zaballa, F. Moreno, B. L. Maroto, J. Bañuelos, I. García-Moreno and S. de la Moya, Multichromophoric COO-BODIPYs: an advantageous design for the development of energy transfer and electron transfer systems, *Chem. Commun.*, 2020, **56**, 13025–13028.

23 (*a*) T. Förster, 10th Spier memorial lecture. Transfer mechanisms of electronic excitation, *Discuss. Faraday Soc.*, 1959, **27**, 7–17; (*b*) G. D. Scholes, K. P. Ghiggino, A. M. Oliver and M. N. Paddon-Row, Through-Space and Through-Bond Effects on Exciton Interactions in Rigidly Linked Dinaphthyl Molecules, *J. Am. Chem. Soc.*, 1993, **115**, 4345–4349; (*c*) S. Speiser, Photophysics and Mechanisms of Intramolecular Electronic Energy Transfer in Bichromophoric Molecular Systems: Solution and Supersonic Jet Studies, *Chem. Rev.*, 1996, **96**, 1953–1976.

24 For example, see: X. Kong, L. Di, Y. Fan, Z. Zhou, X. Feng, L. Gai, J. Tian and H. Lu, Lysosome-targeting turn-on red/NIR BODIPY probes for imaging hypoxic cells, *Chem. Commun.*, 2019, **55**, 11567–11570.

25 H. Tanaka, Y. Inoue and T. Mori, Circularly Polarized Luminescence and Circular Dichroisms in Small Organic Molecules: Correlation between Excitation and Emission Dissymmetry Factors, *ChemPhotoChem*, 2018, **2**, 386.

26 J. Jiménez, F. Moreno, B. L. Maroto, T. A. Cabreros, A. S. Huy, G. Muller, J. Bañuelos and S. de la Moya, Modulating ICT emission: a new strategy to manipulate the CPL sign in chiral emitters, *Chem. Commun.*, 2019, **55**, 1631–1634.

